This paper proposes a method of modeling the dynamic properties of multi-valley semiconductors. The model is applied to the relevant materials GaN, AlN, and InN, which are now known by the general name of III-nitrides. The method is distinguished by economical use of computational resources without significant loss of accuracy and the possibility of application for both dynamic time-dependent tasks and the fields variable in space.

The proposed approach is based on solving a system of differential equations, which are known as relaxation ones, and derived from the Boltzmann kinetic equation in the approximation of relaxation time by the function of distribution over k-space. Unlike the conventional system of equations for the concentration of carriers, their pulse and energy, we have used, instead of the energy relaxation equation, an equation of electronic temperature as a measure of the energy of the chaotic motion only. Relaxation times are defined not as integral values from the static characteristics of the material but the averaging of quantum-mechanic speeds for certain types of scattering is used. Averaging was carried out according to the Maxwellian distribution function in the approximation of electronic temperature, as a result of which various mechanisms of dispersion of carriers are taken into consideration through specific relaxation times. The system of equations includes equations in partial derivatives from time and coordinates, which makes it possible to investigate the pulse properties of the examined materials. In particular, the dynamic effect of the "overshoot" in drift velocity and a spatial "ballistic transport" of carriers.

The use of Fourier transforms of pulse dependence of the drift carrier velocity to calculate maximum conductivity frequencies is considered. It has been shown that the limit frequencies are hundreds of gigahertz and, for aluminum nitride, exceed a thousand gigahertz

Keywords: III-nitrides, dispersion mechanisms, relaxation, ballistic transport, dynamic characteristics, limit frequency

UDC 621.382
DOI: 10.15587/1729-4061.2021.225733

MODELING THE DYNAMIC PROPERTIES OF III-NITRIDES IN STRONG ELECTRIC FIELDS

K. Kulikov*
E-mail: kvprint@gmail.com
V. Moskaliuk
PhD, Professor*
E-mail: v.moskaliuk@gmail.com
V. Timofeyev
Doctor of Technical Sciences, Professor,
Head of Department*
E-mail: v.timofeyev@kpi.ua
*Department of Electronic Engineering
National Technical University of Ukraine "Igor Sikorsky
Kyiv Polytechnic Institute"
Peremohy ave., 37, Kyiv, Ukraine, 03056

Received date 05.01.2021
Accepted date 15.02.2021
Published date 26.02.2021

1. Introduction

Nitride semiconductors in recent years have been of great interest [1–3] due to their exceptional properties that have not been detected in conventional semiconductors such as silicon and gallium arsenide. For example, the prohibited region of the latter is not large enough for the design of optoelectronic devices of the shortwave spectrum [4–6], or devices for ultra-fast signal transmission, for example [7–9]. Moreover, gallium arsenide-based devices cannot be used at high temperatures [10].

Technological development of gallium nitride [11] significantly pushed not only silicon devices in the field of ultra-high frequency and ultra-fast-performance devices but also devices based on gallium arsenide. The logical next step is to study other nitrides with semiconductor properties, namely aluminum nitride, and indium nitride. Recently, the scientific literature [12] uses the generalized name of all three materials – "III-nitrides", which emphasizes their belonging to both nitrogen compounds and the well-known semiconductor group $A^{III}B^{V}$.

Group III nitrides due to the wide prohibited zone can be used in devices of purple, blue, and green radiation spectra [13], as well as for high-temperature transistors. Higher values of working intensity of the electric field and increased thermal conductivity give hope for the creation of a wide range of microwave and EHF powerful devices.

Model approach [14] was used to study the electronic and energy properties of modern semiconductor materials [15], the mechanisms for dispersion of carriers in a strong electric field to increase the efficiency of devices have been elucidated.

Particular attention is paid to the study of frequency characteristics of III-nitrides in strong fields. In particular, the effects of electronic gas heating, and other effects inherent in such materials when they reach nano dimensions. Comparison with the results of experiments and studies by other specialists is given in [16, 17].

Fundamental physical-mathematical principles for modeling modern semiconductor materials were created. An improved method of relaxation equations [18] was used, where the equation for electronic temperature is used instead of the energy balance equation. The times of relaxation of pulse and electron energy for different mechanisms of dispersion were used. For III-nitrides, inter-valley scattering was considered through certain types of scattering on acoustic and optical phonons, since they are distinguished by a wide phonon prohibited zone. When modeling complex compounds, the method can naturally take into consideration the times of relaxation for scattering on the alloy deformation potential.

A method of analysis of frequency conductivity capabilities of material based on a Fourier transform dependent on the pulse reaction of drift velocity [19, 20] was considered. Pulse capabilities of compounds associated with the effect of a "burst" in the drift electron velocity in a strong electric

field were also studied. This effect refers to the so-called quasi-ballistic phenomena and makes it possible to obtain picosecond current pulses as a reaction to switching the voltage on, which creates a strong electric field.

Practical semiconductor devices use various physical phenomena [3, 6, 8] and mechanisms [4, 9], which requires a model acceptable both when changing the intensity of the electric field in time and spatial changes in the volume of semiconductor material. It is also promising to use the Fourier transform of the pulse dependence of the carrier drift rate to calculate the maximum frequencies inherent in the semiconductor. The main advantage of this approach is that it is not necessary to limit the search for maximum frequencies with additional conditions.

2. Literature review and problem statement

Starting with the description of the first GaN-based transistor [21] practical studies of III-nitrides [11–13] continue, which have not yet been completed [1, 3].

A successful attempt to build a model in terms of the possibilities of calculating important parameters for real devices, most researchers consider [11]. The study was a logical continuation of GaAs experiments and contains a thorough comparison with this most studied semiconductor material. Without denying the contributions of the author's collective [11], we should note the following:

– the presence of two types of the crystal lattice of each of III-nitrides was not taken into consideration at all;

– they used redundant and costly method of Monte Carlo;

– calculations in the time and spatial variables of strong electric fields require separate calculations;

– the value of inter-valley phonon is taken the same as optical.

Further experiments [12, 13, 15] prove that inter-valley scattering can also cause acoustic phonons near the edge of the Brillouin zone, so the energy of inter-valley phonons should be chosen as some average for optical and acoustic shortwave phonons. In addition, longitudinal and transverse phonons, in particular for hexagonal structures, take part in phonon dispersion mechanisms. Since the generally accepted dissipation theories do not consider its anisotropy, doubtful consideration of only longitudinal phonons can be compensated by taking into consideration the energy of phonons, as the average of the entire spectrum of optical branches.

There is a request to predict the maximum conductivity frequencies required in the development of modern semiconductor devices [4–9]. The new model for III-nitrides proposed in work [22] is not limited to the possibility of describing electronic transport but allows the analysis of dynamic characteristics.

In [23], numerical modeling by the Monte Carlo method for the alternating electric field, the limit frequency by the standard of achieving the largest efficiency on the first current harmonica for multi-valley semiconductors is determined. Practical use of this method for III-nitrides is given in [17, 24, 25]. Each of the experiments focuses on a separate of the III-nitrides. But at its core, such calculations are possible only under the mode of limiting the accumulation of volumetric charge (LAVC). In this mode, there is no dependence of the frequency of oscillations of the circuit on the time of electrons flying through the diode and, accordingly, on its size. It is clear that the criteria for the existence of LAVC have restrictions both from below (the oscillation period should be greater in order to have time for the formed domain to disappear) and from above (the period is less than the time of relaxation). Thus, the results reported in [17, 24, 25] can be used for qualitative evaluation of other models, in particular the distribution of characteristics between different nitrides.

Another study [10] offers an example of a well-studied GaAs estimate of the maximum frequency provided that negative differential conductivity exists (hereinafter referred to as NDC). The approach was adapted for GaN [26] and even taking into consideration different types of the crystal lattice. It is clear that the assessment by this method is naturally inherent only in the presence of the NDC regime.

Thus, the problem of building and verifying the working model of maximum conductivity frequencies of III-nitrides in strong fields is relevant and needs to be solved [15].

3. The aim and objectives of the study

The purpose of this study is to develop a numerical model of conductivity in multi-valley semiconductors in strong electric fields. This would make it possible to predict the parameters and characteristics of actual semiconductor devices without costly full-time experiments or to recommend the material to the requirements of the device.

To accomplish the aim, the following tasks have been set:

– economical use of computational resources compared to the Monte Carlo method;

– to check matches with existing experimental data;

– to ensure applicability to fields variable both in time and space;

– to use the resulting model for new and promising semiconductors with sufficient accuracy for practical use in the development of finished products.

4. Materials and methods to study multi-valley semiconductors

Compounds considered in this work are a group of nitrides, the properties of which condition their wide use in gadgets and devices for various technical purposes. The group of III-nitrides belongs to compounds of the $A^{III}B^{V}$ type, which are formed as a result of the interaction of elements from subgroup III of the periodic table such as boron, aluminum, gallium, and indium with such an element of subgroup V as nitrogen.

Within each group of compounds, there is a decrease in the width of the prohibited zone with an increase in the total atomic number and atomic masses of the elements included in the compound. This is due to the stronger blurring of the "electron clouds" of covalent bonds as it moves down the periodic table, whereby the metallic nature of the bond is enhanced. Simultaneously with the weakening of covalent chemical bonds, the melting point and hardness of the material decrease, that is, the semiconductor becomes more plastic [27].

This is illustrated in Fig. 1, where, for the cubic structure of the crystal lattice, there are the surfaces corresponding to the position of the bottom of the conductivity zone at points of symmetry Γ, L, and X, built according to the data given in works [28, 29]. It should be noted that the mutual location of the Γ-, L-, and X-valleys may vary depending on the chemical composition. The indium and gallium connections are straightforward semiconductors (except GaP). Compounds of aluminum and gallium phosphide have the bottom of the conductivity zone at point *X*.

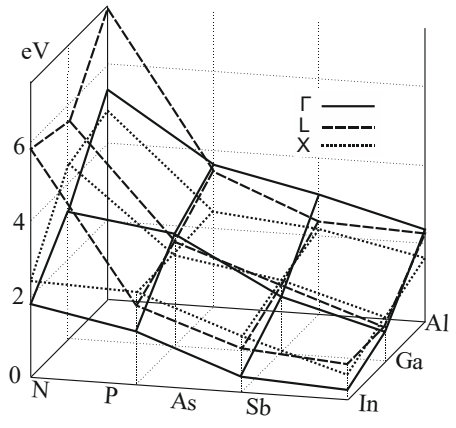

Fig. 1. Dependence of the width of the prohibited zone at different points of symmetry (Γ, L, and X) in the Brillouin zone on the composition of the connection

Group III-nitrides, unlike most compounds of $A^{III}B^{V}$, which crystallize only in a cube-type lattice, can have another modification of the crystalline structure – hexagonal and the structure of rock salt.

For the face-centered cubic lattice [15], as well as a diamond, the first Brillouin zone takes the shape of an octahedron with cut vertices (Fig. 2, *a*). Its symmetry makes it possible to set the law of dispersion only within 1/64 of the Brillouin zone.

The structure of hexagonal type is also characteristic of nitrides (Fig. 2, *b*). In the lattice of both types, each atom of the element from group III is surrounded by the tetrahedron of the four atoms of the group V element, and vice versa. The structure of sphalerite, unlike the structure of a diamond, does not have a center of symmetry. This feature leads to a difference in the properties of surfaces [111] and [110], entirely composed of various atoms. The different behavior of faces is manifested during etching, oxidation, and when growing crystals.

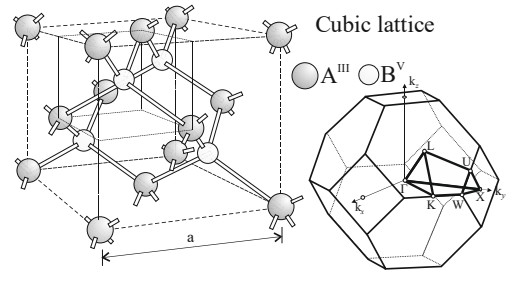

a

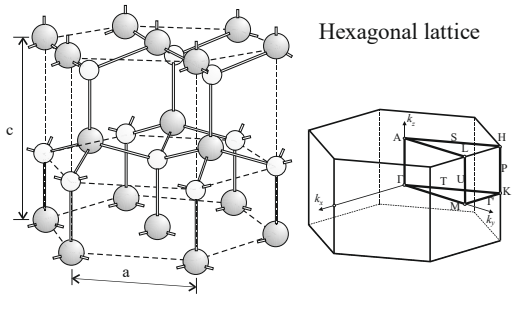

b

Fig. 2. The structure of the crystal lattice and the shape of their first Brillouin zone: *a* – cubic; *b* – hexagonal

As a rule, for group III nitrides, the conduction zone consists of several sub-zones with a minimum in the center of the Brillouin zone $k_{<000>}$ and crystallographic directions <111>, <100>. The minimum is in the center zone – Γ-valley, in the <100> and <111> directions, respectively, X- and L-valley. The exception is aluminum nitride with a cubic modification of the crystal lattice. It is a non-indirect semiconductor and has a minimum, not in the center of the Brillouin zone but in the <100> crystallographic direction, that is, in the X-valley $\Delta_{\Gamma L}$, $\Delta_{\Gamma X}$, Δ_{XL} are the energy gaps between valleys. At the same time, which of the minima is absolute in size depends on a specific compound. The width of the prohibited zone is defined as the smallest, in terms of energy, the distance between the highest point of the valence zone and the lowest energy value of the bottom of the conductivity zone – E_g. When the valley bottom is located near the edge of the Brillouin zone, there are three equivalent X-valleys, four – equivalent to the L-valley. When the bottom of the valleys is in the middle of the Brillouin zone, there are six equivalent X-valleys, eight – equivalent L-valleys. Each of the valleys is characterized by an effective mass of electrons near the bottom of the zone m_Γ, m_X, m_L.

The valence zone consists of two sub-zones that are matched at k=0 and one lower zone grafted as a result of a spin-orbital interaction. Processes in the valence zone have little effect on the effect of inter-valley electron transfer and, therefore, are not considered.

The most common for simulation is the choice of the energy of optical phonons, corresponding to the branch of longitudinal optical phonons (LO) in the center of the Brillouin zone. But shorter-wave phonons also take part in scattering on optical deformation potential. As for the inter-valley phonons, for example, in [11], modeling by the Monte Carlo method employed their value that is the same as the optical ones. But inter-valley scattering can also cause acoustic phonons near the edge of the Brillouin zone, so the energy of inter-valley phonons is usually chosen as some average for optical and acoustic shortwave phonons. Another note can be made regarding participation in the phonon mechanisms of dispersion of longitudinal and transverse phonons, especially for hexagonal structures. Since in generally accepted dissipation theories its anisotropy is not considered, it is possible to express doubts about taking into consideration only longitudinal phonons and choose the energy of phonons as the average of the entire spectrum of optical branches.

The material parameters are taken mainly from review articles [28, 29] and books [30, 31]. The collected paramek ters for further modeling are given in Table 1.

These parameters are sufficient for further modeling and take into consideration the features of the zone structure and types of the inherent crystal lattice. It should be noted that in the reference literature sometimes there is significant uncertainty in the values of some constants. This applies primarily to inter-valley distances, acoustic and optical deformation potentials, inter-valley constants, as well as the values of effective masses.

Electronic temperature determines the main relaxation parameters of the electronic collective of semiconductors and, therefore, their kinetic and dynamic parameters, such as mobility, reaction to pulse and high-frequency fields, etc. The issue of heating electronic gas in multi-valley semiconductors has been discussed for a long time [32], such studies were carried out mainly by the numerical method of Monte Carlo. A thorough analysis of the depen-

dence of the time of relaxation of impulse and energy on the electronic temperature in [18] was limited to only one valley, and, in that analysis, some averaged temperature for valleys was used.

Table 1

Recommended parameters for modeling

Parameter	InN		GaN		AlN	
	cubic	hexa.	cubic	hexa.	cubic	hexa.
Dielectric permeability:						
static, ε_{st}	14.86	15.3	9.6	8.9	8.41	9.14
high-frequency, ε_{hf}	8.04	9.3	5.5	5.35	5.32	4.84
medium, ε	11.0	12.2	9	6.5	7.5	7.2
Ionization energy, eV	0.005		0.013		0.019	
Density, 10^3 kg/m^3	6.81		6.15		3.26	
Sound speed (longitudinal), 10^3 m/s	5.2	6.56	4.57	6.56	6.56	
Acoustic deformation potential, eV	5.0	4.1	5.0	8.3	9.4	8,0
Inter-valley connection constant, 10^{10} eV/m	8	10	11.1	10	11.1	
Optical phonon energy, eV	0.03	0.057	0.059	0.073	0.062	0.055
Inter-valley phonon energy, eV	0.041	0.073	0.05	0.05	0.08	0.08
Inter-valley distance, eV	$\Delta_{\Gamma X}$=0.57 $\Delta_{\Gamma L}$=3.88 Δ_{LX}=3.31	$\Delta_{\Gamma A}$=0.7 $\Delta_{\Gamma\Gamma 1}$=1.1 $\Delta_{\Gamma 1A}$=0.4	$\Delta_{\Gamma X}$=1.1 $\Delta_{\Gamma L}$=1.9 Δ_{XL}=0.6	$\Delta_{\Gamma 1LM}$=2.1 $\Delta_{\Gamma 1\Gamma 2}$=1.9 $\Delta_{\Gamma 2LM}$=0.2	$\Delta_{\Gamma X}$=1.1 $\Delta_{\Gamma L}$=4.4 Δ_{LX}=3.3	$\Delta_{\Gamma ML}$=0.7 $\Delta_{\Gamma K}$=1.0 Δ_{MLK}=0.3
Effective mass: lower valleys	0.64m 0.64m 0.64m	0.4m 0.5m 1.09m	0.15m 0.15m 0.15m	0.2m 0.21m 0.45m	0.17m 0.2m 0.25m	0.14m 0.45m 0.55m
upper valleys	0.48m 0.41m 1.16m	0.8m 1m 3.5m	0.35m 0.36m 1.7m	0.35m 0.91m 2.7m	0.6m 0.65m 2.8m	0.8m 1m 2.8m

The main relaxation parameters of the electronic collective of semiconductors, and, therefore, their kinetic and dynamic parameters, such as mobility, reaction to pulse and high-frequency fields, and the like, are modeled mainly by the numerical method of Monte Carlo. The method has information redundancy and does not make it possible to obtain analytical ratios. This also applies to such a well-known [10] dynamic phenomenon as an "overshoot" of drift speed. An attempt to apply in [11] for its modeling the relaxation equations cannot be fully recognized as successful. Probably the reason for this is the incorrect use of those equations and the finding of relaxation times.

The usual form of relaxation equations for impulse and energy, derived from the averages of the Boltzmann kinetic equation, takes the following form

$$d\vec{p}/dt - e\vec{\mathscr{E}} = -\vec{p}/\tau_p, \quad (1)$$

$$dE/dt - e\vec{v}\vec{\mathscr{E}} = -(E-E_0)/\tau_E. \quad (2)$$

Here, τ_p and τ_E are, respectively, the times of relaxation of impulse and energy, determined from static field-speed and field-temperature characteristics, as it is performed in [11], or from analytical ratios obtained from averaging the speeds of different scattering mechanisms [18, 33].

For multi-valley semiconductors, equations (1) and (2) must be solved for each valley, and the results should be averaged taking into consideration the distribution of electrons across the valleys. The dynamics of valley population is determined by the following equation for concentration in the i-th valley

$$dn_i/dt = -n_i/\tau_{nij} + n_j/\tau_{nji} \quad (3)$$

and analogous equations for the j-th valley

$$dn_j/dt = -n_j/\tau_{nji} + n_i/\tau_{nij}, \quad (4)$$

where τ_{nij} and τ_{nji} are the concentration times of inter-valley relaxation, which can be found using the time of relaxation of the impulse during inter-valley scattering [33].

The second circumstance that must be borne in mind when using equation (2), and which was not taken into consideration in [11], is that the energy E includes both the energy of the chaotic thermal motion E_t, and the energy of the directed drift motion $E_d = m^* v^2/2$, which in strong fields are measured in size.

Drift motion energy is determined by the pulse balance equation (1), from which, by multiplying by drift velocity, is easy to obtain the balance equation for drift energy

$$dE_d/dt - e\vec{v}\vec{\mathscr{E}} = -2E_d/\tau_p. \quad (5)$$

Subtracting (5) from (2), we derive the following equation of the thermal energy balance only

$$\frac{dE_t}{dt} = -\frac{E_t - E_0}{\tau_E} + \frac{E_d}{\tau_E}\left(\frac{2\tau_E}{\tau_p} - 1\right), \quad (6)$$

which describes the degree of heating of electrons. Here, $E_0=3k_bT/2$ is the equilibrium thermal energy, $2\tau_E/\tau_p \equiv \gamma$ is a parameter that determines the efficiency of the transition of drift energy to heat and depends on the degree of collisions' non-plasticity. For electron temperature, which is a measure of chaotic motion energy $E_t=3k_bT_e/2$, equation (6), taking into consideration that the drift speed $v = \mu E = (e\tau_p/m_c^*)E$, takes the following form

$$\frac{dT_e}{dt} = -\frac{T_e - T}{\tau_E} + \frac{m^*\mu^2\mathscr{E}^2}{3k_b\tau_E}(\gamma - 1). \quad (7)$$

In a static field, equation (7) is converted to the following equality

$$\frac{T_e}{T}-1=\frac{m^*\mu^2\mathcal{E}^2}{3k_b}(\gamma-1), \tag{8}$$

which determines the field-temperature characteristics, that is, the connection of electron temperature and intensity of the electric field. The calculation of temperature as a function of intensity in an explicit form is complicated due to the complex dependence of the time of relaxation of impulse and energy on the electron temperature.

Here it should be noted that the reverse relaxation times in each valley are found by summing up the reverse times for different scattering mechanisms. The average mobility in the valleys and the ohmic effective mass are determined for a two-valley model from the following ratios

$$\mu=b_i\mu_i+b_j\mu_j, \tag{9}$$

$$1/m^*=b_i/m^*_i+b_j/m^*_j, \tag{10}$$

where $b_i\equiv n_i/(n_i+n_j)$, $b_j=1-b_i$ are the normalized concentrations (valley population). To find them, it is necessary to use equations (3) and (4).

The average time of pulse relaxation in the valleys is found, as always, from the field-speed characteristics, or from resulting mobility

$$\tau_p=\mu m^*/e, \tag{11}$$

and the average time of energy relaxation, unlike [11], from a field-temperature characteristic

$$\tau_E=\tau_p/2+3k_B(T_e-T)/2\,\mu\mathcal{E}^2. \tag{12}$$

The described equations were used to simulate the effect of "overshoot" in aluminum nitride, gallium, and indium of hexagonal and cubic modifications, the initial parameters of which, in addition to the energy of phonons, were chosen the same as in [11]. For a time-based jumping electric field, changing from zero to a fixed value, time dependences of speed, electronic temperature, time of relaxation, valley population were calculated. Speed time dependence was transferred to spatial via the following integration

$$x=\int_0^t v(t)\,\mathrm{d}t. \tag{13}$$

For high-frequency changes in the electric field, we shall limit ourselves to the calculation of the so-called low-signal conductivity. To this end, all variables $a(t)$ were given as the sum of a constant component a_0 and a small harmoniously variable in time with an amplitude $a_\sim$: $a(t)=a_0+a_\sim e^{i\omega t}$. Neglecting the terms of the second-order of smallness and given that $\partial/\partial t=i\omega$, the equations used were divided into time-independent for constant components and linear equations for the amplitudes of variables.

The use of such a procedure for current density $j=env$ makes it possible to obtain such a ratio to calculate its high-frequency component

$$j_\sim=en_0v_\sim+ev_0n_\sim. \tag{14}$$

Hence, one can see that the alternating component of the current is determined by two factors: variable speed and variable concentration of electrons due to inter-valley transitions. Accordingly, high-frequency conductivity for each valley includes two terms. By computing $v_\sim$ and $n_\sim$ as proportional to the variable amplitude of the electric field $\varepsilon_\sim$, we obtain two characteristic terms for conductivity.

For the first term, in accordance with (14), the result can be represented as follows:

$$\sigma_\omega^{(1)}=\frac{\sigma_0}{1+i\omega\tau_{p0}}\left[1-\frac{v_0}{v_N}\cdot\frac{1}{1+i\omega\tau_{E0}}\right]. \tag{15}$$

If we assume that the conductivity value is determined mainly by the electrons of one valley, then (15), at $\omega\to0$, coincides with the formula describing low-frequency differential conductivity.

The second term, defined by the variable component of the concentration of electrons, as an addition to (15) for high-frequency electrical conductivity

$$\sigma_\omega^{(2)}=-\frac{e^2n_0\tau_{p0}}{m^*}\cdot\frac{v_0}{v_N}\cdot\frac{\tau_{E\omega}}{\tau_0}\cdot\frac{b_{i0}b_{j0}}{1+i\omega\tau_E}\cdot\frac{\Delta_{ji}}{kT}. \tag{16}$$

Here, the concept of the total time of inter-valley relaxation is introduced through inverse times of relaxation between individual valleys

$$\tau_{mm}=\left(1/\tau_{ij0}+1/\tau_{ji0}\right)^{-1} \tag{17}$$

The value of high-frequency electrical conductivity, normalized by its static value, can be calculated from the following ratio

$$\frac{\sigma_\omega}{\sigma}=\frac{\tau_{p\omega}}{\tau_{p0}}-\frac{v_{0\Gamma}}{v_{pN\Gamma}}\cdot\frac{\tau_{E\omega}}{\tau_0}\left(\frac{\tau_{p\omega}}{\tau_{m0}}+\frac{b_{i0}b_{j0}}{1+i\omega\tau_E}\cdot\frac{\Delta_{ji}}{kT}\right). \tag{18}$$

An important result of the above analysis is the possibility of calculating the maximum frequency of existence of negative differential conductivity (NDC). It can be carried out by neglecting the inertia of inter-valley transitions $(\omega\tau_m\ll1)$, by late collisions $(\omega\tau_p\ll1)$, and believing that under the mode of NDC the speed of electrons reaches saturation $(v_{0d}=v_{nd})$. Then formula (18) is simplified and takes the following form:

$$\frac{\sigma_\omega}{\sigma}\approx1-\frac{1-i\omega\tau_{E0}}{1+\omega^2\tau_{E0}^2}\left(1+b_{i0}b_{j0}\frac{\Delta_{ji}}{k_bT_e}\right). \tag{19}$$

Hence, the condition Re $\sigma_\omega=0$, which corresponds to the limit situation, easily produces

$$\omega_m\tau_{E0}=\sqrt{b_{i0}b_{j0}\Delta_{ji}/k_bT_e}. \tag{20}$$

At the field intensity when the populations of the upper and lower valleys are the same and the value of NDC is maximum, the last expression is simplified and the limit frequency is

$$f_m=\frac{1}{4\pi\tau_{E0}}\sqrt{\frac{\Delta_{ji}}{k_bT_e}}. \tag{21}$$

Fig. 3 shows that the limit frequency, which is determined mostly by the time of relaxation of energy, takes a value of the order of hundreds or even thousands of gigahertz, decreasing with increasing intensity of the electric field.

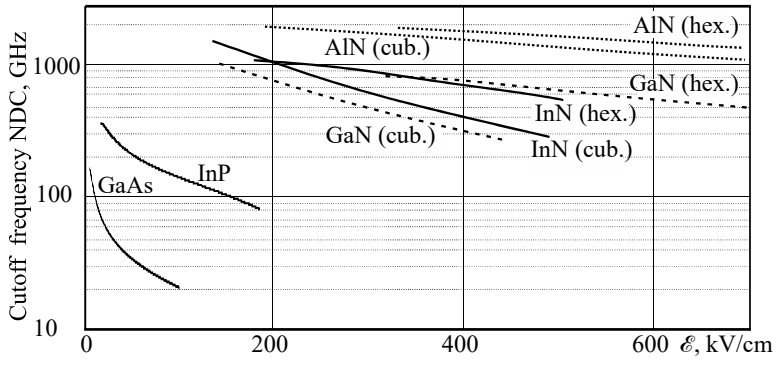

Fig. 3. Dependence of the maximum frequency of NDC existence for III-nitrides on the intensity of the electric field. For comparison, the dependences for GaAs and InP are given

An interesting trend is observed for nitrides with the cubic structure of the lattice – the dependence of the limit frequency on the intensity of the electric field is shifted towards smaller field values. Although for critical fields the limit frequencies for them are somewhat larger, for the mode of greatest negative differential conductivity, these frequencies are almost the same.

Our results for the limit frequency, in a general case, correspond to the results reported in [23] but, for gallium nitride, significantly exceed the results of the forecast given in [34].

While maintaining the practical applicability of the above method [22], we propose to consider an additional approach [19].

The assumptions made when assessing the limit frequency of NDC existence may not be fulfilled for some semiconductors, for example, with a short inter-valley distance. Alternatively, the frequency properties of the semiconductor can be clarified due to the reaction of the drift carrier velocity to the pulse action of the electric field. The proposed approach is based on solving a system of differential equations, which is composed of relaxation equations to conserve energy, impulse and carrier concentration relative to relaxation times for different types of scattering.

The proposed method is based on the Fourier-spectrum analysis of the pulse reaction of the carrier drift velocity in a semiconductor material, the frequency limit assessment. In addition, it is possible to compare with the results beyond the existence of negative dynamic conductivity [22]. Strictly speaking, the test pulse should be an δ -similar pulse of the intensity of the electric field, but, to determine the maximum frequencies chosen for the target of the experiment, the situation is naturally simplified. If we take into consideration the phenomenon of "overshoot" of drift velocity, the most high-frequency components of the Fourier transform take place on the front of the transition process.

5. Results of research into the dynamic properties of III-nitrides

5. 1. Using an economical calculation model

With the help of (2), (5) and an expression to take into consideration the population of valleys in the two-valley approximation, a system of differential equations was built, in the same way as in [20]. The mathematical analytical form of the equation system is adapted for calculations using the Mathcad software package and is solved by the Runge-Kutta IV-order method.

The results of calculations are shown in Fig. 4–9 in the following sequence: time of relaxation of impulse and energy (Fig. 4–9, *a*), field-speed characteristic (Fig. 4–9, *b*), the population of valleys (Fig. 4–9, *c*). The dynamic population reactions (Fig. 4–9, *d*) and drift velocity (Fig. 4–9, *e*) are calculated for a rectangular field pulse. On the spatial manifestation of the effect of "overshoot" (Fig. 4–9, *f*) in hexagonal lattices, for comparison, the results of calculations using the Monte Carlo method from work [11] are inserted. The points on the curves (Fig. 4–9, *e*) correspond to the values of the pulse relaxation times for the specified field intensity. The intensity values of the field for which the simulation was carried out were chosen the same as in [11], the highest values are 3–5 times higher than the critical values.

The results of calculations that are given in Fig. 4–9 demonstrate that in the initial section, electrons under the action of $e\mathscr{E}$ force accelerate; the ballistic movement is observed with a linearly increasing speed $(e\mathscr{E}/m^*)t$. The distance traveled by ballistic motion increases parabolically Such movement continues over the time of order τ_p for a weak field, after which, as a result of scattering, the movement parameters are relaxed to the values characteristic of drift motion in a given strong field. Comparison of Fig. 4–9, *e* and inserts in them in Fig. 3–8 demonstrates a much smaller difference in the results obtained by the Monte Carlo method and the method of relaxation equations than those shown in Fig. 5 borrowed from work [11]. It is obvious that the reason for this difference is the incorrect use of equation (1) for full energy by the authors of [11].

Of course, the peak values of the "overshoot" increase with increasing intensity. At the largest values of the field, they are 4–8 times higher than the corresponding stationary values from the field-speed characteristics. The highest absolute speed values were obtained for indium nitride – about $15 \cdot 10^5$ m/s at a much lower field intensity than in other nitrides. This can be explained by the fact that indium nitride has the greatest time of pulse relaxation, and this is the time over which ballistic speed growth continues.

In fact, for the same reason, the length of the "ballistic mileage" is the largest in indium nitride, about 0.1 μm, while for other materials it is almost an order of magnitude smaller.

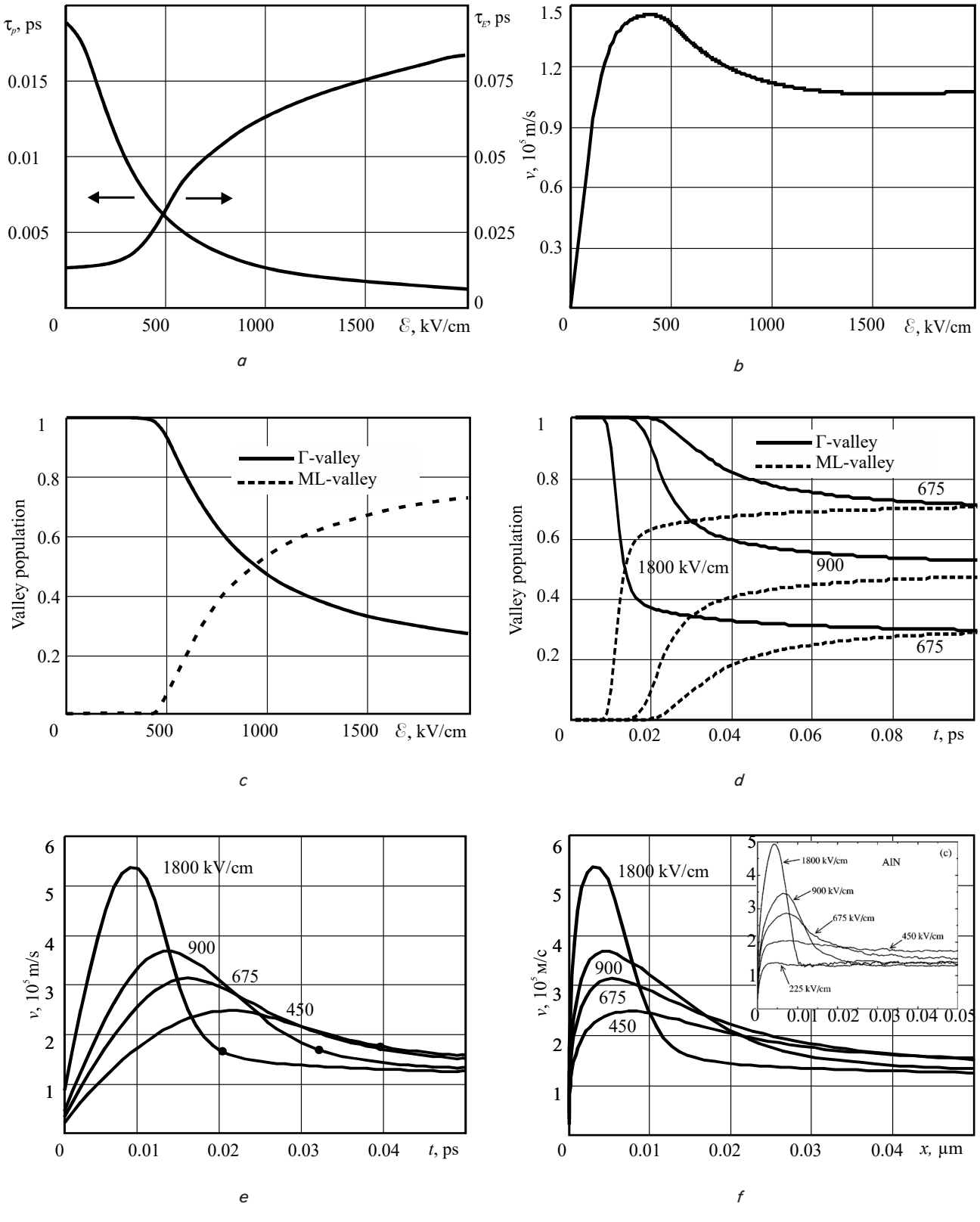

Fig. 4. The results of calculations for aluminum hexagonal nitride:
a — times of relaxation of impulse and energy; *b* — field-speed characteristics;
c — population of valleys. Dynamic reactions: *d* — population;
e — drift velocity (the points on the curves correspond to the values of
the pulse relaxation time for the specified field intensity), calculated for the rectangular pulse of the field;
f — the spatial manifestation of the "overshoot" effect, for comparison:
the results of calculations by the Monte Carlo method from work [11] were inserted

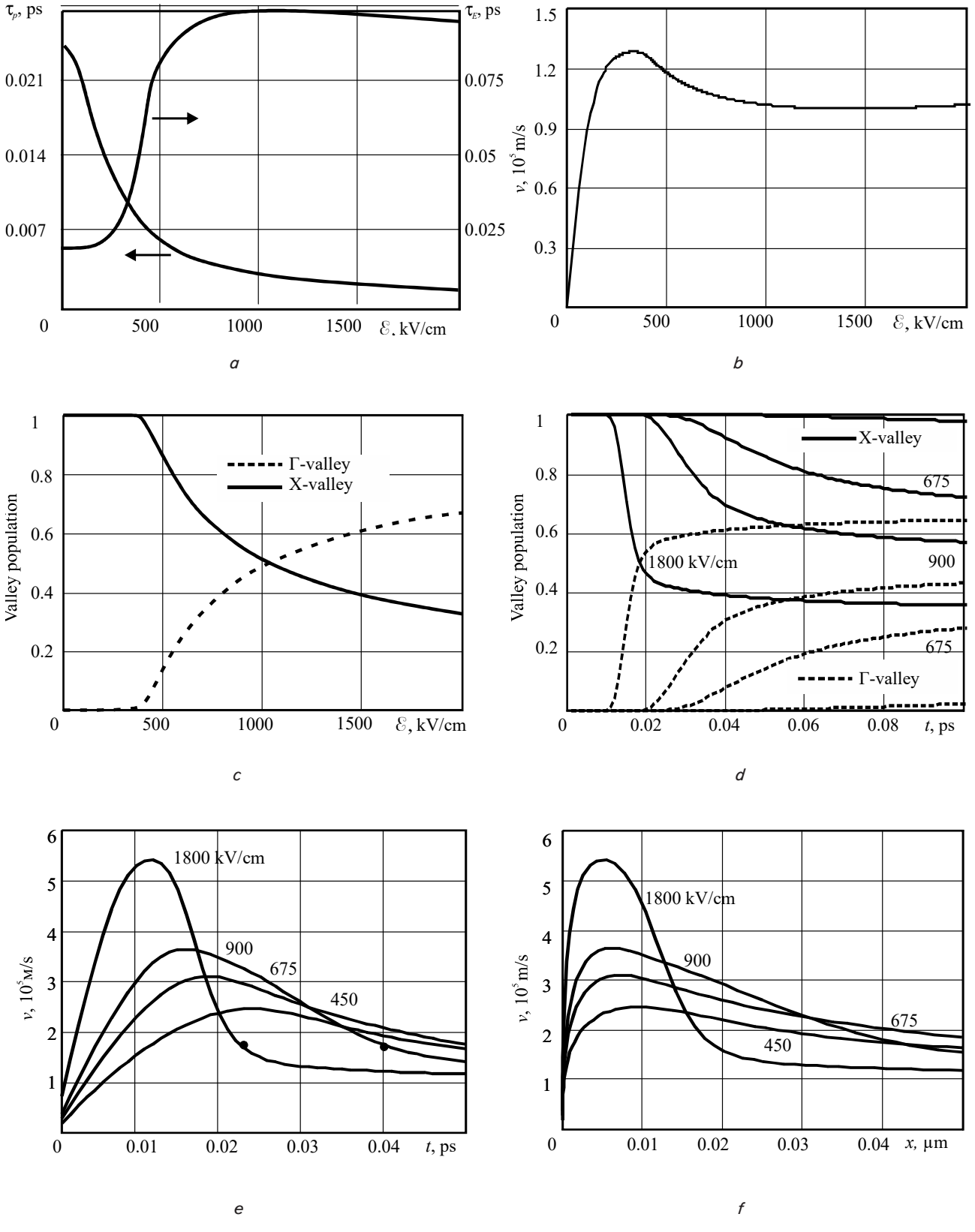

Fig. 5. The results of calculations for cubic aluminum nitride:
a — times of relaxation of impulse and energy;
b — field-speed characteristics; *c* — population of valleys. Dynamic reactions:
d — population; *e* — drift velocity (the points on the curves correspond to the values of
the pulse relaxation time for the specified field intensity), calculated for the rectangular pulse of the field;
f — the spatial manifestation of the "overshoot" effect

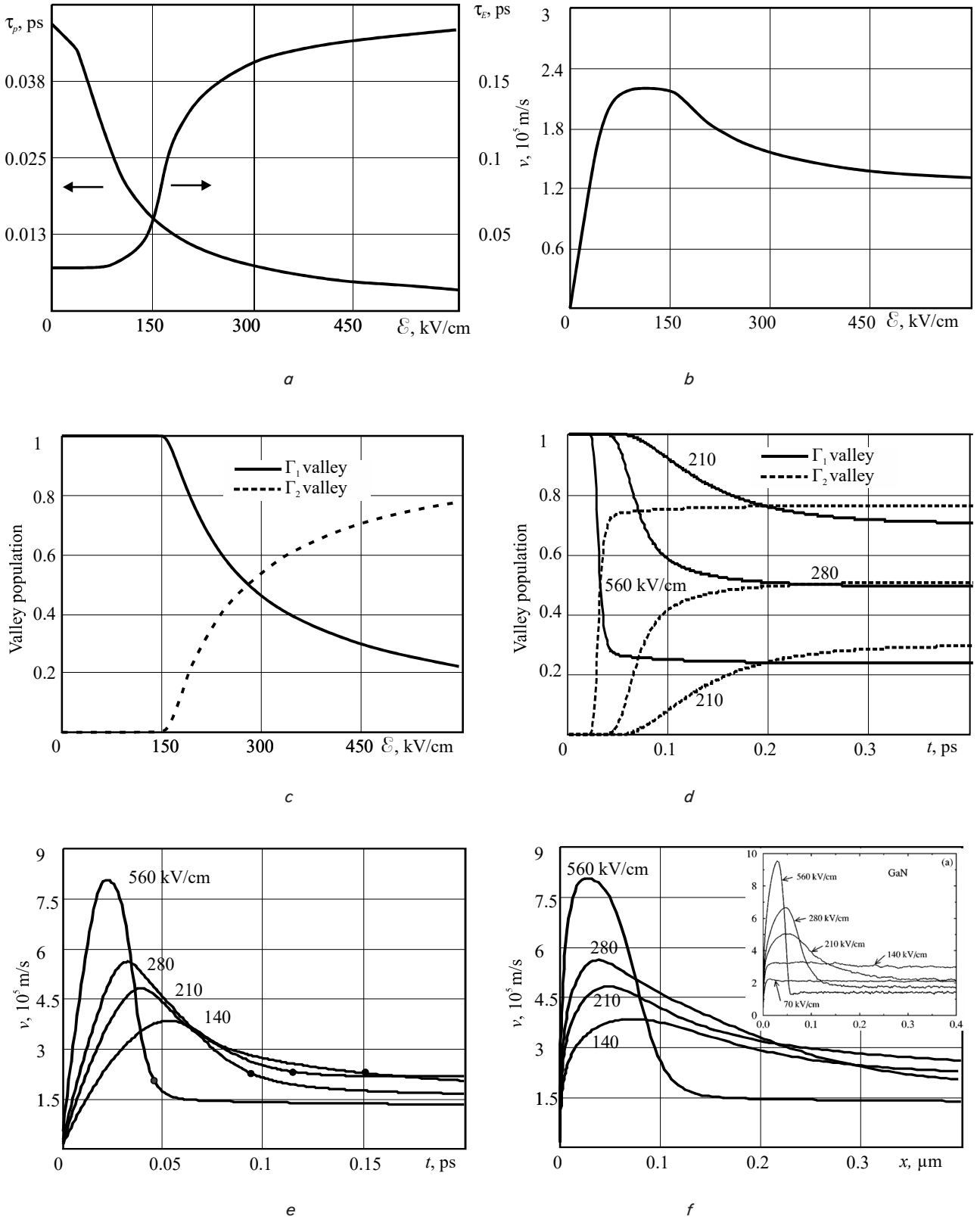

Fig. 6. The results of calculations for hexagonal gallium nitride:
a — times of relaxation of impulse and energy; *b* — field-speed characteristics;
c — population of valleys. Dynamic reactions: *g* — population; *e* — drift velocity (the points on the curves correspond to the values of the pulse relaxation time for the specified field intensity), calculated for the rectangular pulse of the field;
f — the spatial manifestation of the "overshoot" effect, for comparison: the results of calculations by the Monte Carlo method from work [11] were inserted

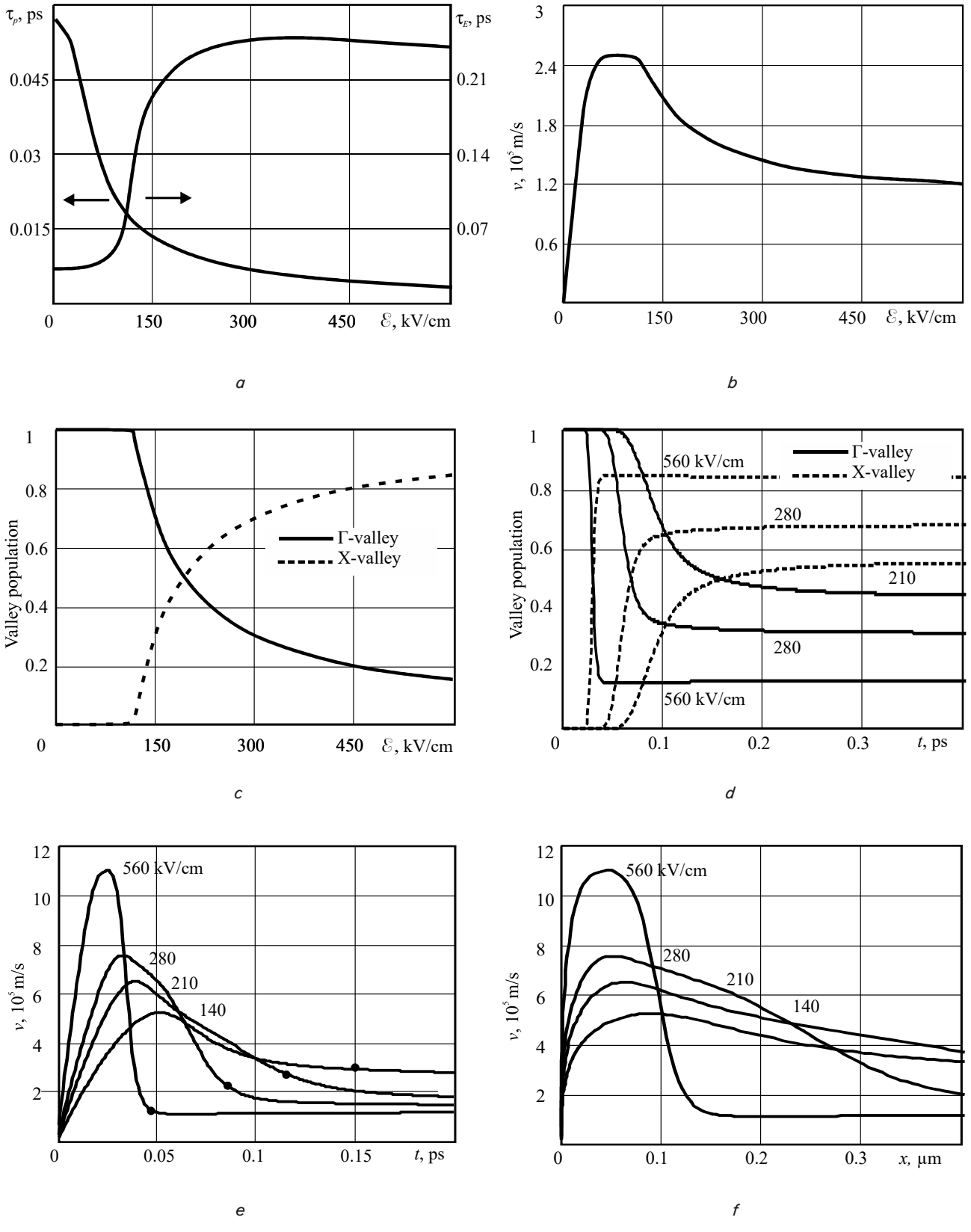

Fig. 7. The results of calculations for cubic gallium nitride:
a — times of relaxation of impulse and energy; *b* — field-speed characteristics;
c — population of valleys. Dynamic reactions: *d* — population;
e — drift velocity (the points on the curves correspond to the values of the pulse relaxation time for the specified field intensity), calculated for the rectangular pulse of the field;
f — the spatial manifestation of the "overshoot" effect

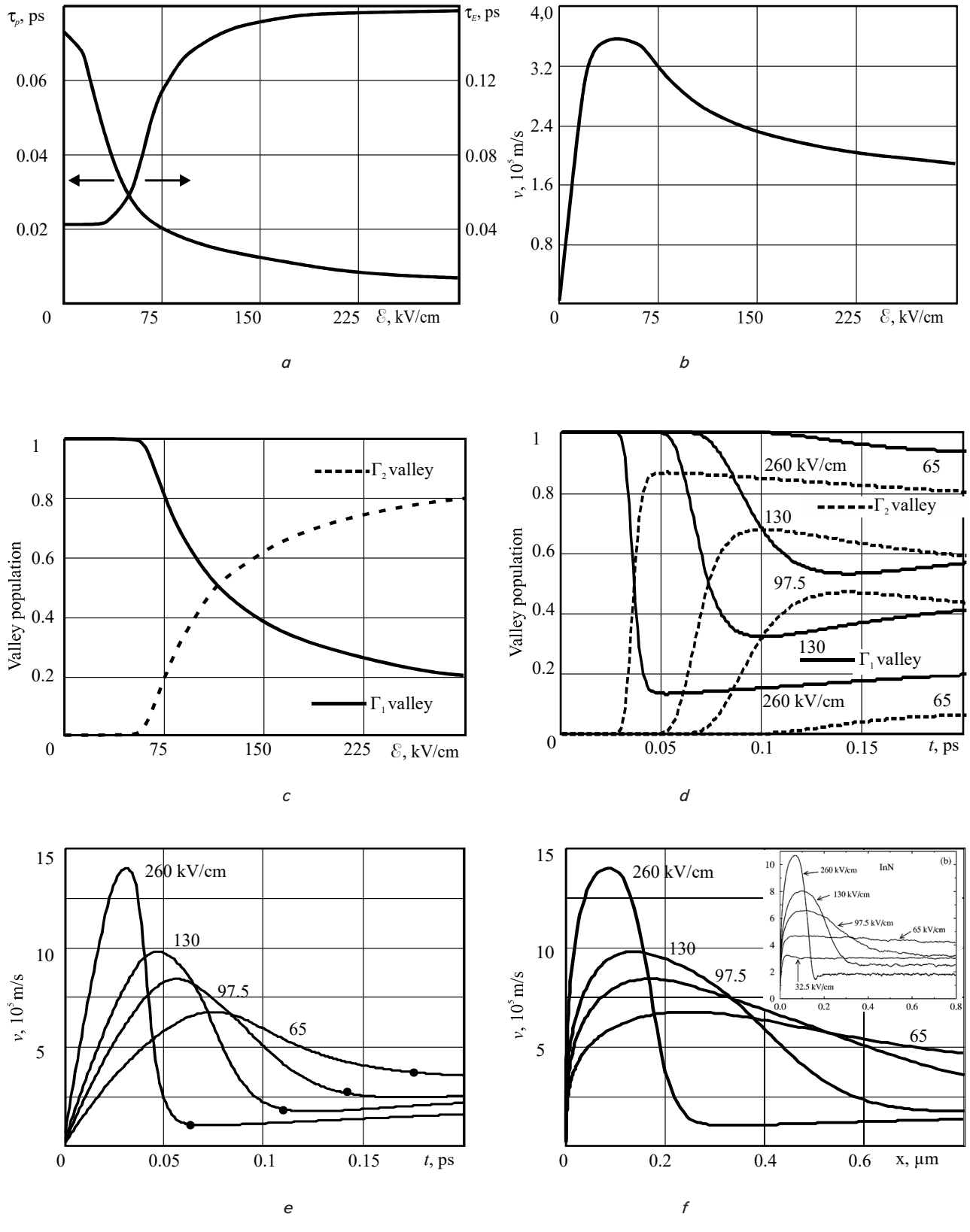

Fig. 8. The results of calculations for hexagonal indium nitride:
a — times of relaxation of impulse and energy;
b — field-speed characteristics; *c* — population of valleys. Dynamic reactions: *d* — population;
e — drift velocity (the points on the curves correspond to the values of the pulse relaxation time for the specified field intensity), calculated for the rectangular pulse of the field;
f — the spatial manifestation of the "overshoot" effect, for comparison:
the results of calculations by the Monte Carlo method from work [11] were inserted

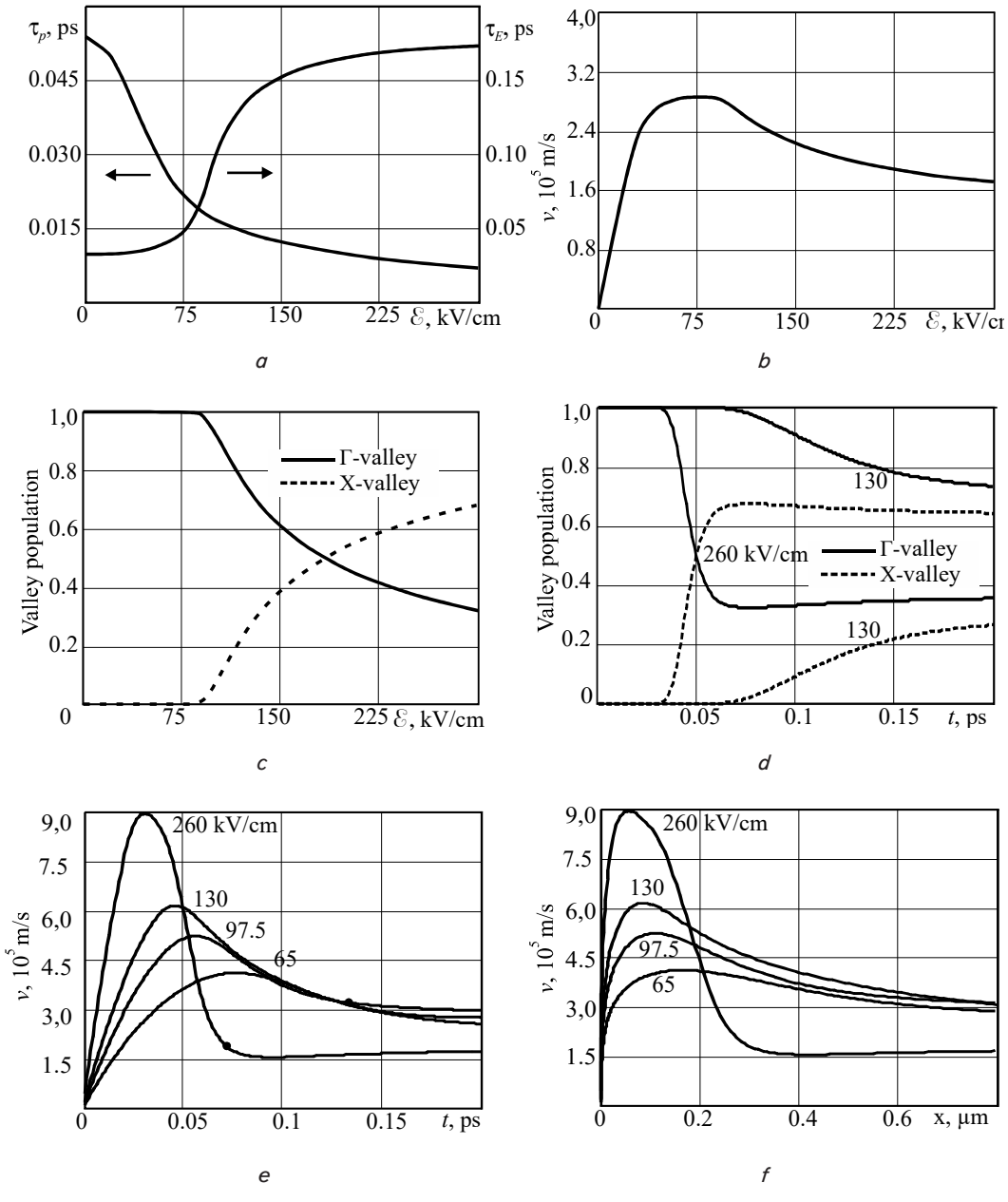

Fig. 9. The results of calculations for cubic indium nitride: *a* – times of relaxation of impulse and energy; *b* – field-speed characteristics; *c* – population of valleys. Dynamic reactions: *d* – population; *e* – drift velocity (the points on the curves correspond to the values of the pulse relaxation time for the specified field intensity), calculated for the rectangular pulse of the field; *f* – the spatial manifestation of the "overshoot" effect

5. 2. Comparing the match with available experimental data

Our results are in good agreement with the results obtained by the Monte Carlo method [11] and indicate that the relaxation equation method is suitable for modeling both static and dynamic properties of semiconductor materials. At the same time, the proposed method, in comparison with the Monte Carlo method, has greater time efficiency and sufficient informativeness.

Separately, it should be noted that the economy of the method implies reducing the time of calculations of the speed of drift carriers in a strong electric field, by an order of magnitude, compared to the Monte Carlo method, on the same equipment and the same input modeling parameters.

5. 3. Applicability to the fields variable both in time and space

The applicability to electric fields variable both in time and space is confirmed by the results shown in Fig. 4–9. In particular, it follows from them that it is possible to use the model simultaneously to determine the drift velocity for the rectangular pulse of the field in time (Fig. 4–9, *e*) and the spatial manifestations of the "overshoot" effect (Fig. 4–9, *f*).

5. 4. Using the model for III-nitrides

The spectral characteristic of the drift velocity obtained by the Fourier transform has been considered. For the possibility of comparison with the results from other experiments

and models, one should dwell on GaN with a hexagonal crystal lattice for a 400 kV/cm electric field.

If we analyze the directly obtained spectral characteristic [26], then two points are worth attention:

1) the "tail" of the spectral characteristic is actually infinite, and demonstrates values much higher than 0 at frequencies up to 10 THz;

2) in the region of 1 THz (in Fig. 10, denoted by a circle), there are unevenness in the fall of spectral density.

Both points are explained by the peculiarities of the Fourier transform; the detailed shape of irregularities depends on the number of sampling points and, accordingly, on the number of stages of approximation.

In work [20], it is proposed to perform a linear approximation of the last "smooth" part of spectral density to the intersection with the abscissa axis. And it is this point of intersection that is considered an estimate of maximum frequency.

The approximation line is represented by a dotted line in the inset in Fig. 10, part *b*. The intersection point with the *x*-axis is marked and is expected in the range of 700–800 GHz.

It is possible to argue about the relevance of this simplification as follows: the slope of the smooth part in a wide range of frequencies corresponds to the physical content of the already formed process, and linear approximation narrows the frequency range, which is enough to assess the "top".

All subsequent images of spectral characteristics are provided with similar approximations. For illustration, the results are given only for one of the III-nitrides – AlN.

The solution to the system for different values of the rectangular impulse of the intensity of the electric field is shown in Fig. 11, 12, *a*.

In the represented analysis, exceeding the carrier drift speeds was observed during pulses lasting up to 0.2 picoseconds. Good agreement with [16] was observed at pulsed velocity characteristics, both for hexagonal and cubic crystal lattices of the III-nitrides studied.

Fourier's rapid transform using 2,048 sampling points was carried out with the above pulsed carrier drift rate responses.

The spectra of pulse velocity are shown in Fig. 11, 12, *b* for both (hexagonal and cubic) lattices of aluminum nitride.

The qualitative analysis of spectral density charts allows us to point to the following.

Comparing the modeling results at different specified values of the intensity of the electric field, one can see a correlation between the corresponding characteristic area on the field-speed characteristics of the carriers and the shape of the chart of the spectral density of Fourier transform. Areas with an ohmic (directly proportional) dependence of the drift velocity on the field are characterized by spectral density curves with clearly defined maxima. Accordingly, the descending area is characterized by monotonous growth of spectral density with a decrease in frequency. This phenomenon manifests itself differently for different semiconductors in fields of varying intensities. Thus, for indium nitride, for almost all curves there is a maximum, but the curves for cubic and hexagonal crystal lattices for values greater than 100 kV/cm differ marks edly in shape. However, for gallium nitride, the phenomenon is observed only up to 100 kV/cm for cubic and, practically, up to 150 kV/cm, for hexagonal crystals. Accordingly, for aluminum nitride, it is up to 500 kV/cm and up to 600 kV/cm.

Since different typical areas of field-speed characteristics are characterized by the different predominance of certain types of scattering, at first glance it seems the counterintuitive effect of the dispersion mechanism on spectral properties. But, realizing that each type of carrier dispersion has its own relaxation time and, accordingly, its frequency of collisions, it is easy to understand that the correlation demonstrated is possible.

The typical shape of these curves for strong fields is the almost constant values of spectral density in the low-frequency part and its decline in the direction of frequency increase. To determine the limit frequencies under these conditions, it is necessary to select additional criteria or simplification procedure to limit the mathematically non-finite spectrum. The use of linear approximation of inclination in the high-frequency area is proposed. The intersection point of the approximating part with the abscissa axis can be considered as an estimate of the frequency of the maximum material for the selected field values. Such an assessment seems quite appropriate and sufficient simplification. This criterion is applied to all spectral characteristics, both with highs and with relatively unchanged spectra.

The resulting linear approximation is denoted by dashed lines in Fig. 11, 12.

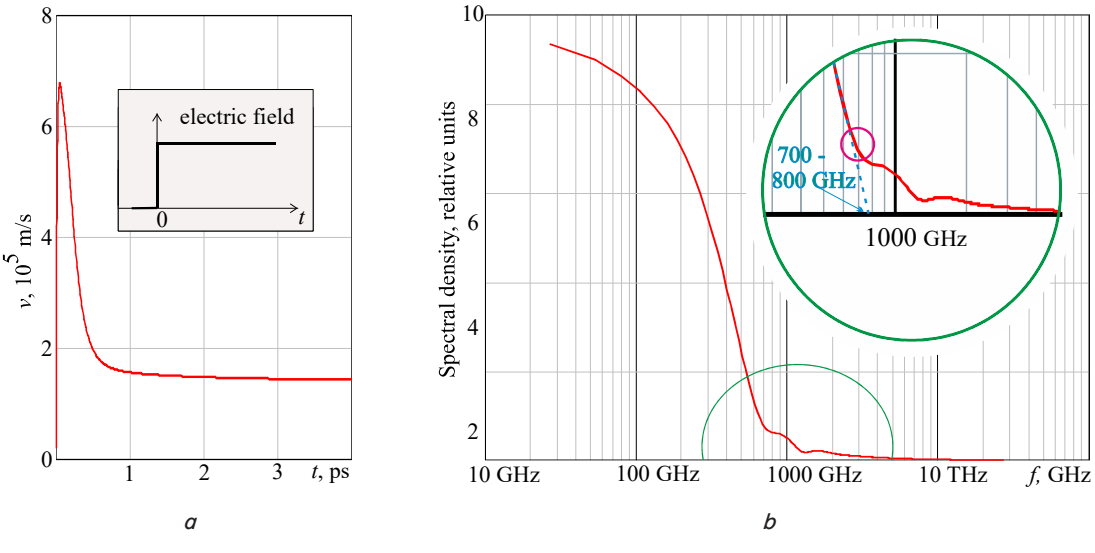

Fig. 10. Pulse and frequency characteristics of GaN with hexagonal crystalline structure: *a* – pulse reaction of drift velocity for 400 kV/cm electric field amplitude; *b* – appropriate spectral characteristics

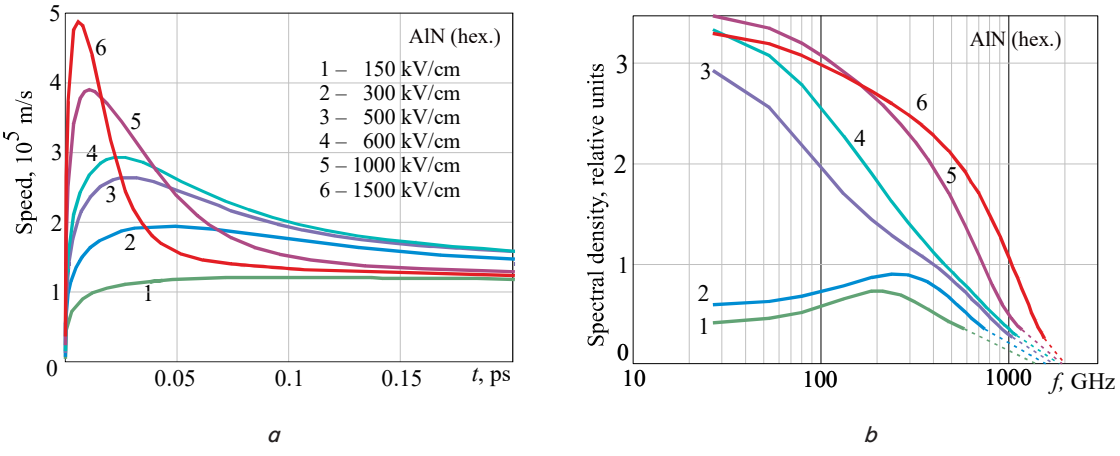

Fig. 11. Crystal structure of AlN of the hexagonal type: *a* – pulse reactions of drift velocity; *b* – spectral characteristics of drift velocity for different values of electric field amplitude

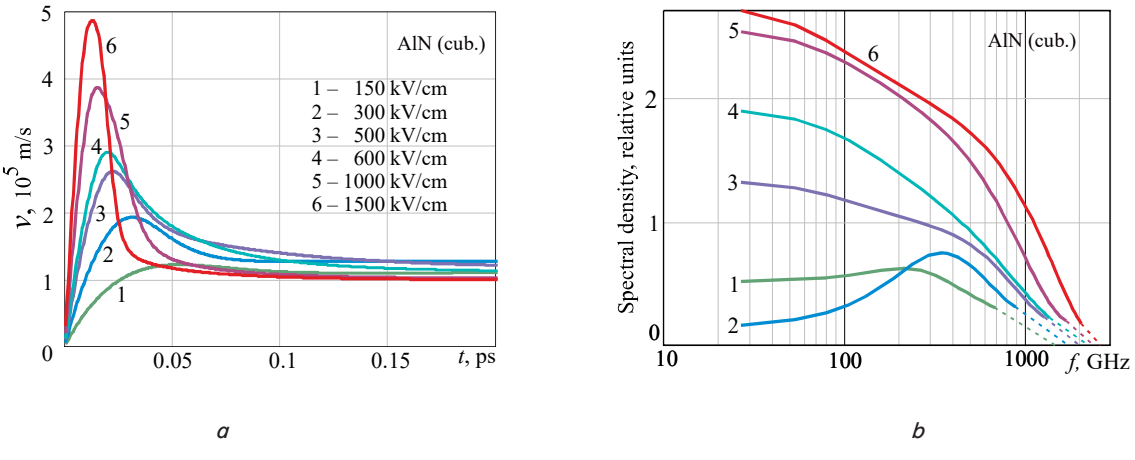

Fig. 12. The crystalline structure of the cubic type AlN: *a* – pulse reactions of drift velocity; *b* – spectral characteristics of drift velocity for different values of electric field amplitude

6. Discussion of results of studying the maximum frequencies of III-nitrides

The frequencies at which the abscissa axis intersection is predicted are grouped and given in Table 2.

Table 2

Maximum frequencies of III-nitrides at different values of the electric field

$\mathcal{E}$, kV/cm	f, GHz					
	InN (cubic)	InN (hexa.)	GaN (cubic)	GaN (hexa.)	AlN (cubic)	AlN (hexa.)
20	400	350	400	400	–	–
50	450	400	450	550	–	–
150	600	550	550	600	1,050	1,040
300	800	800	650	800	1,075	1,060
500	1,020	1,030	900	950	1,100	1,070
600	1,050	1,060	1,000	1,020	1,120	1,080
1,000	–	–	–	–	1,130	1,090
1,500	–	–	–	–	1,150	1,100

However, for a more direct and understandable comparison with Fig. 3, namely with the frequency of negative dynamic conductivity existence, it is more appropriate to investigate Fig. 13.

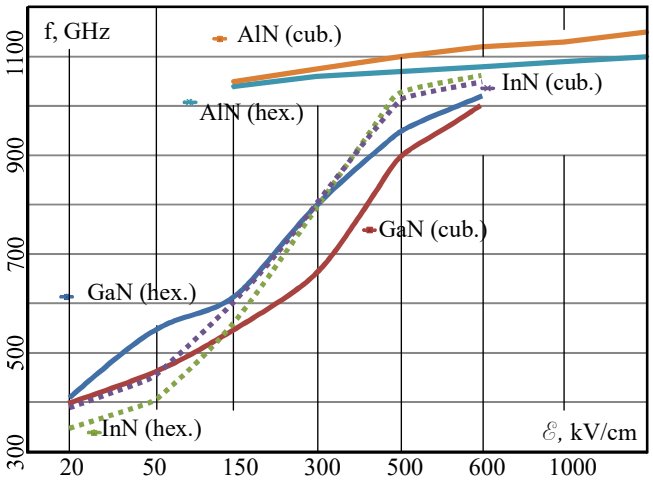

Fig. 13. Maximal frequencies of GaN, AlN, and InN

Fig. 13 clearly demonstrates the prospects of developing devices using AlN with sufficient development of material manufacturing technology.

Comparing the results using Fourier transform and the maximum frequency of the existence of NDC allows us to draw the following conclusions:

a) AlN is the most promising according to both methods, but the type of the "fastest" crystal lattice is different. This is a promising topic for additional research and search for new experimental data;

b) the general nature of dependences differs. The conditions of NDC existence reduce the maximum frequencies with increasing intensity of the electric field. The "overshoot" of drift velocity increases depending on the amplitude of the field, which leads to an increase in the estimate of the maximum frequency. From a physical point of view, there is no contradiction, since different mechanisms and criteria of existence are employed;

c) the overall mutual location of dependences for different III-nitrides coincides, which indirectly confirms the validity of the proposed model and its forecasts in previously non-studied ranges of external conditions.

Based on our study, the features related to the following have been established:

a) the movement of carriers of III-nitrides in strong electric fields variable both in time and space;

b) the distribution of the concentration of carriers in valleys depending on the electric field;

c) the patterns of pulse conductivity, which, in turn, has made it possible to perform a comparative analysis of various methods for estimating the boundary frequencies of multi-valley semiconductors and to offer a new one, which is characterized by ease of calculations, agreement with the results from other experiments, and a larger range of possible values of the external electric field.

This model has limitations because it is built in the so-called two-valley approximation when the law of dispersion considers processes in the lowest valley and the nearest higher ones. This is the case in the $A^{III}B^{V}$ binary compounds, which are considered in the current paper. In triple compounds, which are binary alloys, there is a change in the position of zones depending on the stoichiometric composition; usually, one needs to use a three-valley model. However, such a model can be obtained by modifying the two-valley model and be considered as the development of the above research results.

To add to the calculations of upper limit frequencies, not only if NDC exists or under the mode of generation in the Hahn diode, the spectral characteristics of the response of drift velocity to various amplitudes of pulses of the electric field, for which we obtained limit frequencies for various materials exceeding the value of 1,000 GHz, especially for aluminum nitrides, were studied. Interestingly, the effect of the dispersion mechanism on spectral properties has been noticed. But, given that each type of scattering has its own relaxation time and, accordingly, its frequency of collisions, it is easy to understand that such a correlation is natural.

Additionally, it should be noted that the topology, manufacturing technology, defects in materials, etc. of actual devices certainly affect the frequency capabilities of the finished product. This leads to the conclusion that the model proposed in this study makes it possible to assess the prospects and applicability of the material under other equal conditions.

7. Conclusions

1. We have proposed a method for modeling the dynamic characteristics of multi-valley semiconductor materials of the $A^{III}B^{V}$ group, which is based on a kinetic equation with model simplifications in relaxation approximation; that makes it possible to solve actual tasks of forecasting the parameters and characteristics of actual devices based on multi-valley semiconductors without costly full-time experiments, or to choose a material according to the customer's requirements for the device. The method is suitable for the analysis of electron transport in a strong electric field and makes it possible to simulate dynamic effects specific to submicronic dimensions.

2. The analytical model, the use of relaxation times, and appropriate simplifications allow the economical use of computational resources, which leads to a decrease in the time of calculation of the drift rate of carriers in a strong electric field, by an order of magnitude, compared to the Monte Carlo method, on the same equipment and the same input modeling parameters.

3. An excellent agreement with experiments was demonstrated, both quantitatively (the size of "overshoot", the order of maximum frequencies) and qualitatively (forecasts for the use of materials in accordance with their parameters).

4. The feasibility of the fields, variable both in time and space, is laid down in the architecture of the model due to the use of equations in partial derivatives from time and coordinates. The model has been applied to actually new and promising III-nitrides with an accuracy sufficient for practical use in the development of finished products (to the order of magnitude) when calculating the upper limit frequencies.

References

1. Siddiqua, P., Wang, Y., Shur, M. S., O'Leary, S. K. (2019). Empirical model for the velocity-field characteristics of semiconductors exhibiting negative differential mobility. Solid State Communications, 299, 113658. doi: https://doi.org/10.1016/j.ssc.2019.113658
2. Smolin, V. K. (2016). High-Frequency Microelectronics Based on Silicon Substrate Structures. Journal of Nano and Microsystem Technique,, 18 (11), 713–717. Available at: http://www.microsystems.ru/files/full/mc201611.pdf
3. Encomendero, J., Jena, D., Xing, H. G. (2019). Resonant Tunneling Transport in Polar III-Nitride Heterostructures. High-Frequency GaN Electronic Devices, 215–247. doi: https://doi.org/10.1007/978-3-030-20208-8_8
4. Guo, W., Zhang, M., Bhattacharya, P., Heo, J. (2011). Auger Recombination in III-Nitride Nanowires and Its Effect on Nanowire Light-Emitting Diode Characteristics. Nano Letters, 11 (4), 1434–1438. doi: https://doi.org/10.1021/nl103649d
5. Arafin, S., Liu, X., Mi, Z. (2013). Review of recent progress of III-nitride nanowire lasers. Journal of Nanophotonics, 7 (1), 074599. doi: https://doi.org/10.1117/1.jnp.7.074599

6. Saxena, D., Mokkapati, S., Jagadish, C. (2012). Semiconductor Nanolasers. IEEE Photonics Journal, 4 (2), 582–585. doi: https://doi.org/10.1109/jphot.2012.2189201
7. Maekawa, T., Kanaya, H., Suzuki, S., Asada, M. (2016). Oscillation up to 1.92 THz in resonant tunneling diode by reduced conduction loss. Applied Physics Express, 9 (2), 024101. doi: https://doi.org/10.7567/apex.9.024101
8. Oshima, N., Hashimoto, K., Suzuki, S., Asada, M. (2016). Wireless data transmission of 34 Gbit/s at a 500-GHz range using resonant-tunnelling-diode terahertz oscillator. Electronics Letters, 52 (22), 1897–1898. doi: https://doi.org/10.1049/el.2016.3120
9. Asada, M., Suzuki, S. (2016). Room-Temperature Oscillation of Resonant Tunneling Diodes close to 2 THz and Their Functions for Various Applications. Journal of Infrared, Millimeter, and Terahertz Waves, 37 (12), 1185–1198. doi: https://doi.org/10.1007/s10762-016-0321-6
10. Shur, M. S. (1987). GaAs devices and circuits. Springer, 670. doi: https://doi.org/10.1007/978-1-4899-1989-2
11. Foutz, B. E., O'Leary, S. K., Shur, M. S., Eastman, L. F. (1999). Transient electron transport in wurtzite GaN, InN, and AlN. Journal of Applied Physics, 85 (11), 7727–7734. doi: https://doi.org/10.1063/1.370577
12. Feng, Z. C. (2006). III-Nitride Semiconductor Materials. World Scientific Publishing Co., 440. doi: https://doi.org/10.1142/p437
13. Ohta, H., Okamoto, K. (2009). Nonpolar/Semipolar GaN Technology for Violet, Blue, and Green Laser Diodes. MRS Bulletin, 34 (5), 324–327. doi: https://doi.org/10.1557/mrs2009.94
14. Hockney, R. W., Eastwood, J. W. (1988). Computer simulation using particles. CRC Press, 540.
15. Moskalyuk, V. A., Timofeev, V. I., Fedyay, A. V. (2014). Bystrodeystvuyuschie pribory elektroniki. Ch. 1. LAP LAMBERT Academic Publishing, 240.
16. Adachi, S. (2009). Properties of Semiconductor Alloys: Group IV, III–V and II–VI Semiconductors. John Wiley & Sons, Ltd. doi: https://doi.org/10.1002/9780470744383
17. Bokula, O., Prohorov, E. (2011). Chastotnye svoystva mezhdolinnogo perenosa v nitride galliya. Tehnika i pribory SVCh, 1, 24–28.
18. Seeger, K. (1973). Semiconductor Physics. Springer, 514. doi: https://doi.org/10.1007/978-3-7091-4111-3
19. Kulikov, K., Baida, I., Moskaliuk, V., Timofeyev, V. (2018). Conductance Cutoff of A3B5 Nitrides at High-Frequency Region. 2018 IEEE 38th International Conference on Electronics and Nanotechnology (ELNANO). doi: https://doi.org/10.1109/elnano.2018.8477497
20. Kulikov, K. V., Moskaliuk, V. O., Tymofieiev, V. I. (2019). High-Frequency Properties of GaN, AlN and InN in Strong Fields. Microsystems, Electronics and Acoustics, 24 (3), 20–32. doi: https://doi.org/10.20535/2523-4455.2019.24.3.178841
21. Asif Khan, M., Kuznia, J. N., Bhattarai, A. R., Olson, D. T. (1993). Metal semiconductor field effect transistor based on single crystal GaN. Applied Physics Letters, 62 (15), 1786–1787. doi: https://doi.org/10.1063/1.109549
22. Moskalyuk, V. A., Kulikov, K. V. (2009). Chastotnye svoystva nitrida galliya v sil'nom elektricheskom pole. Visnyk Derzhavnoho universytetu informatsiyno-komunikatsiynykh tekhnolohiy, 7 (3), 306–309.
23. Prohorov, E. D., Beletskiy, N. I. (1982). Poluprovodnikovye materialy dlya priborov s mezhdolinnym perenosom. Kharkiv: Vyscha shkola, 144.
24. Botsula, O. V. (2010). Chastotnye svoystva mezhdolinnogo perenosa elektronov v ALN. Visnyk Kharkivskoho natsionalnoho universytetu imeni V.N. Karazina. Seriya: Radiofizyka ta elektronika, 927 (16), 7–10. Available at: http://ekhnuir.univer.kharkov.ua/bitstream/123456789/7172/2/927-4.pdf
25. Botsula, O. V. (2010). Chastotnye svoystva mezhdolinnogo perenosa elektronov v InN. Visnyk Kharkivskoho natsionalnoho universytetu imeni V.N. Karazina. Seriya: Radiofizyka ta elektronika, 942 (17), 67–70. Available at: http://dspace.univer.kharkov.ua/bitstream/123456789/7206/2/942-10.pdf
26. Kulikov, K., Moskaliuk, V., Timofeev, V. (2017). High-frequency conductance cutoff of gallium nitride. 2017 IEEE International conference of information-telecommunication technologies and radio electronics (UkrMiCo'2017), 317–319.
27. Bonch-Bruevich, V. L., Kalashnikov, S. G. (1990). Fizika poluprovodnikov. Moscow: Nauka, 688.
28. Vurgaftman, I., Meyer, J. R., Ram-Mohan, L. R. (2001). Band parameters for III–V compound semiconductors and their alloys. Journal of Applied Physics, 89 (11), 5815–5875. doi: https://doi.org/10.1063/1.1368156
29. Vurgaftman, I., Meyer, J. R. (2003). Band parameters for nitrogen-containing semiconductors. Journal of Applied Physics, 94 (6), 3675–3696. doi: https://doi.org/10.1063/1.1600519
30. Kasap, S., Capper, P. (Eds.) (2017). Springer Handbook of Electronic and Photonic Materials. Springer, 1536. doi: https://doi.org/10.1007/978-3-319-48933-9
31. Ivaschenko, V. M., Mitin, V. V. (1990). Modelirovanie kineticheskih yavleniy v poluprovodnikah. Kyiv: Naukova dumka, 192.
32. Matulenis, A., Pozhela, Yu., Reklaytis, A. (1978). Dinamika razogreva elektronov. V kn. Mnogodolinnye poluprovodniki. Vil'nyus, 204.
33. Moskaliuk, V. O. (2004). Fizyka elektronnykh protsesiv. Dynamichni protsesy. Kyiv: IVTs Vyd. «Politekhnika», 180.
34. Danilin, V., Zhukova, T. (2005). Tranzistory na GaN poka samiy krepkiy oreshek. Elektronika: nauka, tehnologii, biznes, 26 (4), 20–28.